



Research Article

Co-processing of Atorvastatin and Ezetimibe for Enhanced Dissolution Rate: *In Vitro* and *In Vivo* Correlation

Mona F. Arafa,^{1,3} Rasha A. Alshaikh,^{1,2} Magdy M. Abdelquader,¹ and Gamal M. El Maghraby¹

Received 14 November 2020; accepted 7 January 2021; published online 31 January 2021

Abstract. Development of fixed dose combinations is growing and many of these drug combinations are being legally marketed. However, the development of these requires careful investigation of possible physicochemical changes during co-processing. This requires investigation of the effect of co-processing of drug combination in absence of excipients to maximize the chance of interaction (if any). Accordingly, the aim was to investigate the effect of co-processing of ezetimibe and atorvastatin on drugs dissolution rate. The objective was extended to *in vitro in vivo* correlation. Drugs were subjected to wet co-processing in presence of ethanol after being mixed at different ratios. The prepared formulations were characterized using FTIR spectroscopy, X-ray powder diffraction, differential scanning calorimetry, scanning electron microscopy, and *in vitro* dissolution testing. These investigations proved the possibility of eutectic system formation after drugs co-processing. This was reflected on drugs dissolution rate which was significantly enhanced at dose ratio and 2:1 atorvastatin:ezetimibe molar ratio compared to the corresponding pure drugs. *In vivo* antihyperlipidemic effects of the co-processed drugs were monitored in albino mice which were subjected to hyperlipidemia induction using poloxamer 407. The results showed significant enhancement in pharmacological activity as revealed from pronounced reduction in cholesterol level in mice administering the co-processed form of both drugs. Besides, histopathological examinations of the liver showed marked decrease in hepatic vacuolation. In conclusion, co-processing of atorvastatin with ezetimibe resulted in beneficial eutexia which hastened the dissolution rate and pharmacological effects of both drugs.

KEY WORDS: atorvastatin; ezetimibe; eutectic mixture; antihyperlipidemic; fixed dose combination.

INTRODUCTION

Development of fixed dose combinations is growing with many products being legally marketed. The development of fixed dose combination can provide a tool for preparation of drug-drug co-processed binary systems. Co-processing may result in formation of new crystalline species which may be of co-crystal, salt, or co-amorphous types. Other mixtures may undergo melting point depression forming eutectic mixture (1). These transformations may beneficially or deleteriously affect the dissolution rate and subsequently the bioavailability of drugs in fixed dose combinations. For example, olmesartan medoxamil has been shown to develop stable co-crystal after co-processing with hydrochlorothiazide. Unfortunately, the developed species underwent slow dissolution of drugs. This problem was solved by inhibition of the co-crystallization

process (2). Accordingly, researchers are focusing on investigation of drug-drug co-processing with emphasis on drug candidates for fixed dose combinations (3–5). This research line is promising and may introduce a new benefit for fixed dose combination.

Atorvastatin is a competitive HMG-CoA reductase inhibitor; the drug is a long acting member of statin family which is widely used as antihyperlipidemic agents. Despite of being one of the most successful members of the statin family, atorvastatin is classified as BCS- class II candidate which undergo slow dissolution. The problem is magnified in acidic pH below 4 modulating the bioavailability (6, 7). Multiple approaches have been conducted successfully to enhance the dissolution rate and the oral bioavailability of atorvastatin; these include particle size reduction via micronization (8) or nano-crystal formation (9, 10), crystal structure modification using inactive cofomers via cocrystallization (11) or co-amorphousization (12), solid dispersion formation (13, 14), self-assembled colloidal drug delivery systems (15, 16), and nanotechnology-based approaches via polymeric nanospheres formation (17) or cyclodextrin-based nanospheres (18). Moreover, the pharmacological activity of atorvastatin can

¹ Department of Pharmaceutical Technology, College of Pharmacy, University of Tanta, Tanta, Egypt.

² School of Pharmacy, University College of Cork, Cork, Ireland.

³ To whom correspondence should be addressed. (e-mail: drmona_arafa@yahoo.com; mona.arafa@pharm.tanta.edu.eg)

be augmented by combination with other lipid lowering agents like ezetimibe which exerts its function by different mechanism. A combination of both drugs is legally available in the market.

Ezetimibe is a cholesterol absorption inhibitor that is commonly indicated in combination with statins for augmented lipid lowering effect (19). Ezetimibe exhibits low aqueous solubility and therefore can be classified as dissolution rate limited drug. Accordingly, several techniques have been conducted aiming to enhance the drug dissolution rate. These include solid dispersion and self-micellizing solid dispersions formation (20, 21), self nano-emulsifying drug delivery system (22), and nanocrystallization (23).

Investigations were extended to simultaneously enhance the dissolution behavior of ezetimibe in combination with atorvastatin. These studies employed solid dispersion and amorphous nano-solid dispersion formation in presence of other excipients (24, 25) and self microemulsifying drug delivery system (26). These investigations overlooked possible interaction between the neat drugs.

Accordingly, the objective of current study was to investigate the effect of co-processing of both drugs using ethanol assisted co-grinding. The scope of the study was extended to evaluate the mechanism of enhanced dissolution of both drugs in addition to *in vivo* evaluation of pharmacological activity before and after co-processing.

MATERIALS AND METHODS

Materials

Atorvastatin, ezetimibe, and poloxamer 407 were obtained from Sigma for Pharmaceutical Industries, Egypt. HPLC grade acetonitrile was purchased from BDH, UK. Ethanol, Tween 80, and potassium dihydrogen phosphate were purchased from El Nasr Pharmaceutical Chemicals Company, Cairo, Egypt.

Methods

Preparation of the Tested Formulations

Co-processing of atorvastatin and ezetimibe was achieved using the previously published method (27). In this method, wet co-grinding of atorvastatin and ezetimibe was performed after mixing both drugs at different molar ratios and at fixed dose ratio (Table I). This involved dry mixing of the required ratio using mortar and pestle. Ethanol was added dropwise with continuous grinding until formation of

smooth paste. This procedure consumed 0.9 ml of ethanol for each gram of the formulation. Grinding process was continued till evaporation of ethanol and the formation of flowable particles. These steps were repeated 5 times and finally, the obtained powder formulation was left overnight for complete drying at room temperature before being packed in air-tight containers.

Determination of Drug Content

Known weight of the tested formulation was dissolved in ethanol and was suitably diluted with filtered water before drug quantification using HPLC method. These procedures were repeated in triplicates. The following equation was utilized for calculating the drug content in each formulation:

$$\text{Drug content (\%)} = (\text{Recovered amount}/\text{Theoretical amount}) \times 100$$

Chromatography

Simultaneous quantitative analysis of atorvastatin and ezetimibe was performed using high-pressure liquid chromatographic method. Chromatographic system (Agilent technologies 1260 infinity, DE, Germany) was used and it was equipped with a variable wavelength UV detector (VWD 1260). A full computer controlled automatic sampling system (TCC 1260) was involved. The mobile phase comprised filtered water adjusted to pH 3 with ortho-phosphoric acid and acetonitrile (45:55). This mobile phase was pumped at a rate of 1.2 ml/min. The stationary phase was a reversed phase Intersil® C18 column, 150 mm × 4.6mm (i.d.) with an average particle size of 5 µm (GL Sciences Inc., Tokyo, Japan.). The samples were injected into the system with a volume of 30 µl and drug concentration was quantified at wavelength of 238 nm. Agilent OpenLAB ChemStation software was utilized for data analysis.

FTIR Spectroscopy

The FTIR spectrophotometer (Bruker Tensor 27, Germany) was utilized for recording the FTIR spectra of pure atorvastatin, ezetimibe, and the prepared formulations. The powdered samples were mixed with potassium bromide (spectroscopic grade) and the resulting mixture was compressed into disks using hydraulic press. Spectroscopic scan was performed for each sample in the range of 4000 to 400 cm⁻¹. DLaTGS detector and Opus IR, FT IR spectroscopy software were employed for detection and data analysis respectively.

Powder X-ray Diffraction

The X-ray diffractograms for atorvastatin, ezetimibe, and the tested formulations were collected using PAN analytical X-Ray diffractometer (model X'Pert PRO, Netherlands). The equipment is supplied with secondary monochromator, Cu-Kα radiation (λ = 1.542 Å) operated at 45 KV and current of 35 mA. Data collection is facilitated using X'Celerator detector. Continuous scan mode using 2theta scan axis was

Table I. The Composition of the Prepared Formulations Presented as Molar Ratios

Formulation	Atorvastatin	Ezetimibe
Atorv:Ezet (0.5:1)	0.5 (6.3 mg)	1 (10 mg)
Atorv:Ezet (1:1)	1 (13.64 mg)	1 (10 mg)
Atorv:Ezet (2:1)	2 (27.4 mg)	1 (10 mg)
Dose ratio*	1.5 (20 mg)	1 (10 mg)

*Dose ratio is approximately equal to 1.5:1 molar ratio of atorvastatin and ezetimibe

conducted at ambient temperature with scanning range of 3 to 65° and scanning step size of 0.03°.

Differential Scanning Calorimetry

The thermal analyses of atorvastatin, ezetimibe, and the prepared formulations were conducted using differential scanning calorimeter (DSC-50, Shimadzu, Japan). Accurate amount of sample was loaded into aluminum pan then it was covered with its lid and was crimped using Shimadzu crimper. Thermal analysis was performed with a heating rate of 10°C/min, over a temperature range of 35–300°C. This process was under continuous flow of nitrogen gas at constant rate. TA-50 WSI thermal analysis software was utilized in data collection and analysis. The melting transition (T_m) was measured for each sample.

Scanning Electron Microscopy

Scanning electron microphotographs of atorvastatin, ezetimibe, and the co-processed fixed dose combination were recorded using scanning electron microscope (JSM-5300, JEOL, Tokyo, Japan) that was operated with controllable acceleration voltage (20 kV). The powders were loaded onto the specimen mounting stubs, coated with a thin layer of gold utilizing the sputter coater unit within a coating time of 7 min (JFC-1100E) and examined microscopically.

Dissolution Studies

The dissolution studies were performed using USP 2 (paddle type) dissolution apparatus. FDA dissolution medium for atorvastatin and ezetimibe was utilized. The medium comprised 0.2% w/v Tween 80 solution in 0.05 M phosphate buffer (pH 6.8). The required volume of the dissolution medium (900 ml) was loaded into the dissolution vessels with the temperature of these vessels being adjusted at $37 \pm 0.5^\circ\text{C}$. The paddle of the apparatus was set at a rotation speed of 75 rpm. Test sample (10 mg of ezetimibe, 20 mg of atorvastatin or equivalent to 10 mg of the ezetimibe) was loaded into the dissolution vessel. Dissolution samples (5 ml) were withdrawn at predetermined time intervals (5, 10, 15, 30, 45, and 60 min) and were filtered immediately using a 0.45 μm Millipore filter. To keep constant volume for the dissolution medium and maintain sink conditions, the withdrawn sample was replenished with fresh dissolution medium. The drugs concentration in each sample was quantified by the developed HPLC assay method. Dissolution testing for each powdered sample was conducted in triplicates. The percent cumulative amounts of drug dissolved were plotted as a function of time to produce dissolution profiles. The dissolution parameters including the amount of drug dissolved within the first 5 min (Q5) and the dissolution efficiency (DE) were computed from these profiles. The dissolution efficiency was estimated using the nonlinear trapezoidal rule (28).

In Vivo Evaluation of Antihyperlipidemic Effect

The study utilized 48 albino mice with an average weight of 25 g. The study design and animal handling were performed according to the rules approved by the College

of Pharmacy, University of Tanta Ethical Committee. The mice were fed with standard pellets diet and water and were left to adapt on the laboratory conditions for 1 week before the experiment. Poloxamer-induced acute hyperlipidemia model was employed for this study (29, 30). During the experiment, the animals were divided into six groups (I, II, III, IV, V, VI). Group I served as naïve without treatment with drugs or poloxamer. Group II was reserved as a reference for mice with hyperlipidemia (induced with poloxamer). Group III received atorvastatin aqueous dispersion orally at a dose of 5 mg/kg p.o. and group IV received ezetimibe at a dose of 2.5 mg/kg p.o. Group V received a dispersion of the physical mixture of atorvastatin and ezetimibe (5/2.5 mg/kg p.o). Co-processed atorvastatin and ezetimibe at a dose ratio of 5/2.5 mg was administered to group VI after dispersion in water. For groups III, IV, V, and VI, drugs were administered on daily basis for 2 weeks before poloxamer induced hyperlipidemia. After these 2 weeks, poloxamer 407 solution in sterile normal saline was prepared and injected in a dose of 0.5 gm/kg intraperitoneally for all groups except group I. This dose was selected based on that reported in literatures (31). The mice were sacrificed 24 h after injection and blood samples were collected, centrifuged at 3000 rpm for 20 min and the serum was separated for total cholesterol analysis using biochemical tests. Enzymatic colorimetric method using the commercial reagent (BioMed-Cholesterol-LS) was employed. Accurate volume of serum (10 μl) was added to 1 ml of the reagent that produces a color according to the level of cholesterol and this was assayed using UV-spectrophotometer at wavelength of 546 nm. The concentration of cholesterol in each sample was calculated by measuring a concentration of a standard sample measured by the same colorimetric technique.

The livers of the sacrificed mice were preserved in 10% buffered formalin (pH 7.4) then they were processed in ascending grades of alcohol followed by xylene. After that, they were embedded in paraffin wax and cut for histopathological examination. This method was previously reported (32). These liver sections were stained with hematoxylin and eosin stain (H&E) then they were microscopically examined using light microscope (Leica system provided with DFC Leica camera) to evaluate steatotic marks of the liver samples.

Statistical Analysis

For the estimated dissolution parameters and the results of *in vivo* testing, the significance of the difference between the tested formulations was evaluated using IBM SPSS 20 software. This employed the use of the Kruskal Wallis test followed by Tukey's multiple comparison as post hoc analysis. In addition, the dissolution profiles were compared using similarity factor test (33).

RESULTS AND DISCUSSION

Characterization of the Prepared Formulations

Drug Content

The drug content values for ezetimibe were determined to be 100.5 ± 0.87 , 99.86 ± 2.32 , 99.41 ± 0.76 , and 101.27 ± 4.03

with that of atorvastatin were calculated to be 99.5 ± 0.87 , 100.14 ± 2.32 , 100.59 ± 0.76 , and 98.73 ± 4.03 for the formulations containing atorvastatin and ezetimibe at molar ratios of 0.5:1, 1:1, 2:1, and dose ratio respectively. The recorded drug content values reflect homogeneity of the mixtures as indicated from the closeness to 100% in addition to the very small SD.

FTIR Spectroscopy

FTIR spectroscopy was utilized to assess any possible interaction between ezetimibe and atorvastatin after co-processing. Figure 1 shows the recorded spectra for ezetimibe, atorvastatin, and the prepared formulations. The FTIR spectrum of ezetimibe shows the identical spectral pattern for its main functional groups (Fig. 1). The spectrum shows broad peak at 3442 cm^{-1} which can be assigned to the intermolecular hydrogen bonded O-H stretch. The C=O of lactam ring appeared at 1718 cm^{-1} . The benzene ring C=C stretching vibration was recorded at 1512 cm^{-1} . The peaks recorded at 1083 and 1218 cm^{-1} can be attributed to C-O and C-F stretching vibrations. The O-H bending vibration was recorded at 1404 cm^{-1} and para-substituted benzene ring vibration was recorded at 827 cm^{-1} . The stretching vibrations for C-H groups are seen at 2924 and 2856 cm^{-1} . These peaks assignments were previously reported for ezetimibe (5, 24).

The FTIR spectrum of pure atorvastatin shows the characteristic peaks that indicate the presence of the drug main functional groups (Fig. 1). The spectrum demonstrates a peak at 3448 cm^{-1} which corresponds to O-H stretching vibration. The C-H stretching vibrations were recorded at 2924 and 2968 cm^{-1} . Strong absorption band at 1653 cm^{-1} can be assigned to the stretching vibration of the amide carbonyl group. The bending vibrations of N-H and O-H groups were recorded at 1514 and 1432 cm^{-1} , respectively. The peaks appeared at 1315 , 1216 , and 1103 and can be assigned to the stretching vibrations of C-N, C-F, and C-O groups respectively. Similar spectral pattern was previously recorded for atorvastatin (24, 34).

Co-processing of atorvastatin with ezetimibe at different ratios resulted in spectral patterns that represent the summation of both drugs. This is clear from the presence of the main characteristic peaks that were assigned for atorvastatin and ezetimibe (Fig. 1). This behavior suggests absence of chemical interaction after co-processing. The same behavior was recorded after dry co-grinding of ezetimibe with aspirin (5) and nonsteroidal anti-inflammatory drugs with caffeine (1).

Powder X-ray Diffraction

The diffractograms of ezetimibe, atorvastatin, and the co-processed formulations were recorded and shown in Fig. 2. For ezetimibe, the diffractogram revealed the main diffraction peaks which were recorded at 2θ values of 7.95 , 9.79 , 12.09 , 13.89 , 15.83 , 17.15 , 18.61 , 19.33 , 20.87 , 21.77 , 22.95 , 23.47 , 24.55 , 25.29 , 26.35 , 27.07 , 28.23 , 30.05 , 31.39 , 32.05 , 33.03 , 39.37 , and 43.19° (Fig. 2). This diffractogram agrees with the previously reported data for the same drug and proves its crystalline nature (35).

The diffractogram of atorvastatin shows several distinct diffraction peaks at 2θ values of 6.09 , 9.11 , 9.43 , 10.25 , 10.51 ,

11.83 , 12.17 , 15.23 , 16.97 , 18.29 , 21.53 , 22.65 , 23.23 , 23.63 , 24.49 , 26.31 , 28.29 , 29.09 , 30.47 , 31.87 , 37.29 , and 43.01° (Fig. 2). The presence of such sharp diffraction peaks indicates the drug crystallinity which is previously shown for atorvastatin in other research articles (36, 37).

Co-processing of ezetimibe and atorvastatin at different ratios resulted in diffraction pattern that comprises the main diffraction peaks for both drugs recorded at the same angular positions but with reduced intensity (Fig. 2). This behavior is the same at all the tested ratios. These data indicate no significant change in the crystalline nature of both drugs with only signs of reductions in particle size being noticed as revealed from the reduced peaks intensity. Similar results were recorded previously for ezetimibe and aspirin co-processed form (5).

Differential Scanning Calorimetry

DSC was used to investigate any changes in thermal behavior of ezetimibe and atorvastatin after co-processing. The recorded thermograms are shown in Fig. 3. The thermogram of ezetimibe shows a sharp endothermic peak at a T_m value of 164.5°C attributed to the drug melting with a dehydration endotherm being recorded at 80.38°C (Fig. 3). Similar thermal behavior for ezetimibe was reported in literatures (38, 39).

With respect to atorvastatin, the recorded thermogram shows a main melting transition at T_m value of 159.6°C . This melting transition was followed by broad and weak endothermic peak at a T_m value of 231.4°C reflecting drug decomposition. Another weak endothermic peak was recorded at 92.1°C owing to loss of adsorbed water or dehydration (Fig. 3). This thermal pattern correlates with the published data on atorvastatin (6, 37). The recorded thermal pattern for ezetimibe and atorvastatin proves their crystalline nature and correlates with the data recorded with X-ray diffractometer.

Co-processing of ezetimibe and atorvastatin resulted in a thermal behavior that is different from the thermal pattern of each drug and depended on the ratio of both drugs. For the co-ground system containing atorvastatin and ezetimibe at a molar ratio of 0.5:1, the thermogram revealed an endothermic peak at T_m value of 63.8°C which can be attributed to water loss. Interestingly, the enthalpy of this endotherm was lower than that expected with the corresponding drug highlighting absence of additional solvent bound to the mixture. This indicates evaporation of most ethanol which was used in wet processing. However, accurate determination of residual ethanol is necessary before taking these formulations to any further applications. A main endotherm was recorded at a T_m of 157.7°C . This T_m was detected at a lower T_m value compared to each of atorvastatin and ezetimibe and this was accompanied with the disappearance of the main endotherms of pure drugs. Another broad endothermic peak was recorded at T_m values of 230°C , reflecting the decomposition of atorvastatin. Mixtures containing atorvastatin at higher molar ratios showed the new endotherm with the T_m being around 152.37 – 152.9°C . The decomposition endotherm of atorvastatin was recorded in the same position as before. This pattern reflects possible development of new crystalline species. Taking this finding with the recorded X-ray diffraction results which showed no evidence for new crystalline form, the recorded thermal behavior indicates the possibility of eutectic system formation.

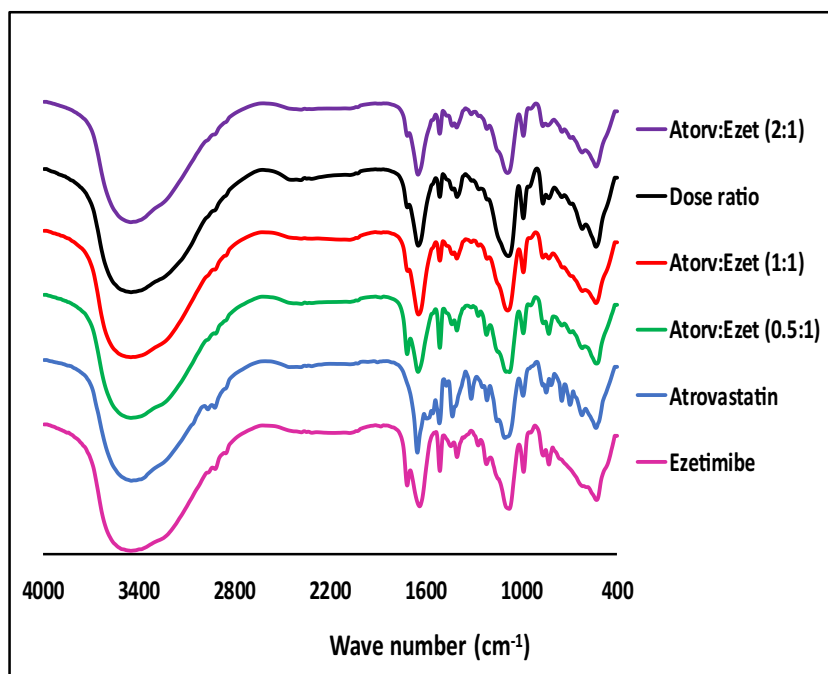


Fig. 1. FTIR spectra of pure unprocessed drugs and the tested formulations

Similar behavior was recorded for other mixtures and was considered as eutectic system by other investigators (1, 40, 41).

Scanning Electron Microscopy

Scanning electron microscopy (SEM) was used to perceive the morphology and size of ezetimibe, atorvastatin, and the co-processed formulation (dose ratio). The recorded photomicrographs are presented in Fig. 4. Atorvastatin crystals appeared as smooth surfaces rod-shaped crystals

accompanied with many irregular shaped particles and slightly agglomerated in bundles (Fig. 4). Similar morphology for atorvastatin powder was depicted previously (24, 37).

The photomicrograph of ezetimibe shows block-shaped crystals which are larger in size compared with atorvastatin crystals (Fig. 4). The same crystal shape was previously recorded for ezetimibe (5, 42).

The co-processed product at dose ratio reflected modulation of the crystalline structure of the product. These changes were shown as a reduction in the crystal size with

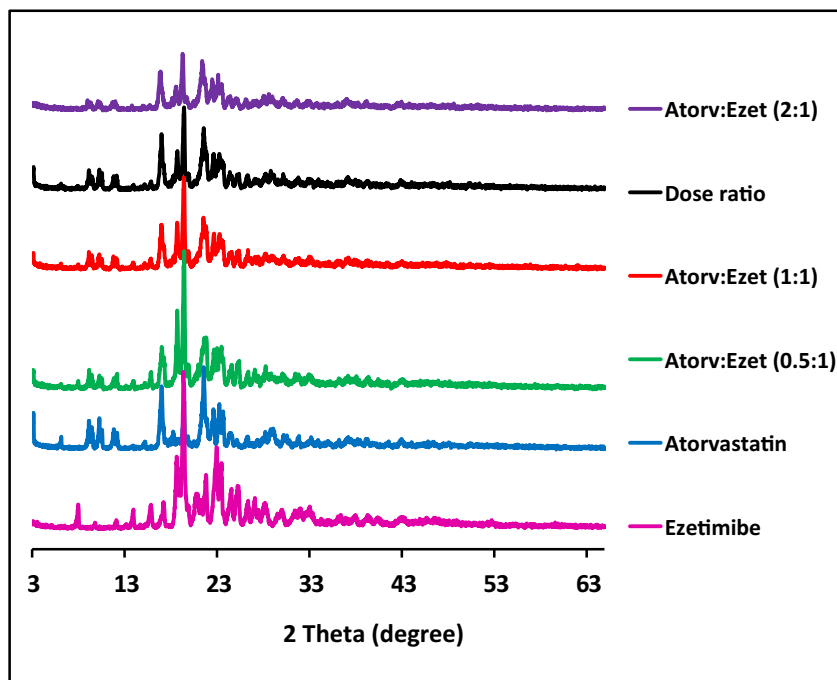


Fig. 2. X-ray diffraction pattern of pure unprocessed drugs and the tested formulations

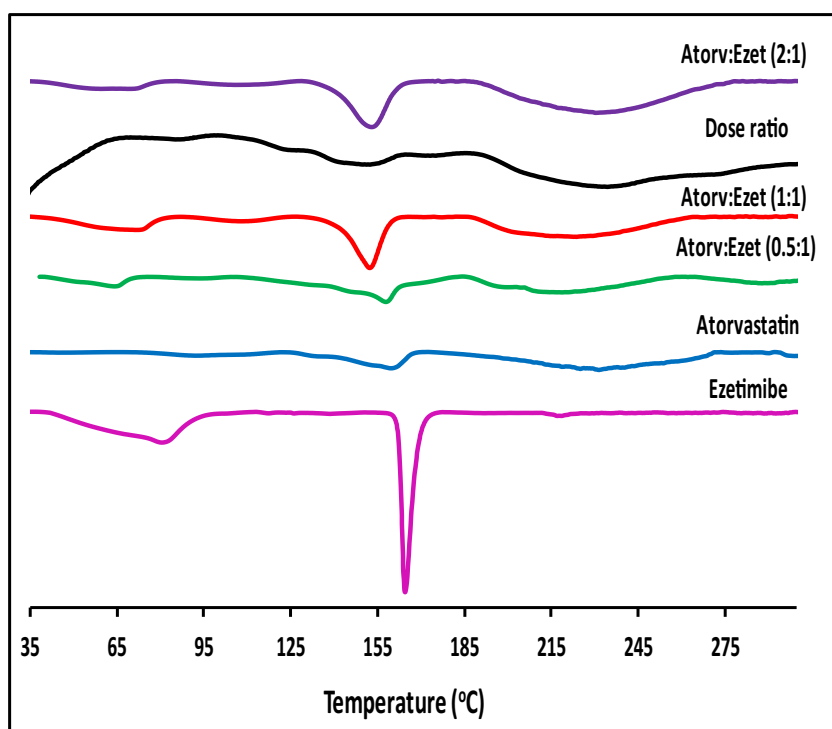


Fig. 3. DSC thermograms of pure unprocessed drugs and the tested formulations

modification of the architecture of the crystals. These changes correlate with the recorded findings of the combined instrumental analysis which supported possible eutectic mixture formation. Similar findings were reported previously and were attributed to eutectic system formation (43, 44).

Dissolution Studies

Dissolution studies were performed to investigate the effect of ezetimibe and atorvastatin co-processing on drugs dissolution rate. The studies were conducted for the co-processed ezetimibe and atorvastatin at different ratios and compared with pure unprocessed drugs. Figure 5 shows the recorded dissolution profiles for both ezetimibe and atorvastatin with the calculated dissolution parameters including overall dissolution efficiency (DE%) and the amount of drug dissolved in the first five minutes (Q5) being shown in Table II.

For ezetimibe, the unprocessed drug showed slow dissolution rate with 16.8% of ezetimibe being dissolved in the first 5 min and 77.6% of the dose (10 mg) was dissolved within 1 h. The overall dissolution efficiency value was calculated to be 51.6% (Table II). This slow dissolution rate for ezetimibe was reported in literatures and was pointed to its hydrophobic nature (35, 45).

The recorded dissolution profile for pure unprocessed atorvastatin revealed Q5 value of 62.9% and overall dissolution efficiency value of 81.3% (Fig. 5 and Table II). This recorded dissolution rate is relatively higher than that reported in literatures using dissolution media without Tween 80, but similar profile was reported in study using dissolution media comprising sodium lauryl sulfate and phosphate buffer (46).

Co-processing of ezetimibe and atorvastatin produced a different dissolution profiles depending on the ratio of both drugs. Co-processing of both drug at molar ratios of 0.5:1 and

1:1 (atorvastatin:ezetimibe) did not result in significant change in the dissolution rate of ezetimibe (Fig. 5a). However, co-processing of atorvastatin and ezetimibe at molar ratios of 2:1 and dose ratio resulted in significant enhancement in ezetimibe dissolution rate with the recorded Q5 values being 85.3 and 75.9% for both ratios respectively.

For atorvastatin, co-processing with ezetimibe at dose ratio resulted in significant enhancement in atorvastatin dissolution rate compared with the unprocessed atorvastatin (Fig. 5b). This enhancement was reflected in the large increase in Q5 and dissolution efficiency values which were recorded to be 90.97% and 91.4% respectively.

The recorded changes in dissolution rate of both drugs after co-processing were evaluated using similarity factor test. The test confirmed similarity between the rate of ezetimibe dissolution from pure unprocessed drug and co-processed forms containing atorvastatin and ezetimibe at molar ratios of 0.5:1 and 1:1 (F2 equal 52 and 76 for both ratios respectively). In contrast, the tests revealed significant increase in the dissolution rate of ezetimibe from formulations containing dose ratio or 2:1 molar ratio of atorvastatin and ezetimibe, compared to unprocessed powder (F2 equal 18 and 13 for both ratios respectively). The similarity factor test confirmed hastened dissolution pattern of atorvastatin after co-processing with ezetimibe at dose ratio (F2 equal 39). The recorded dissolution enhancement can be claimed to be due to melting point depression which resulted in weaker intermolecular forces with subsequent rapid dissolution. Similar behavior has been shown after eutectic mixture formation (1).

In Vivo Evaluation of Antihyperlipidemic Effect

Poloxamer-induced acute hyperlipidemia model was employed to evaluate the effect of oral administration of

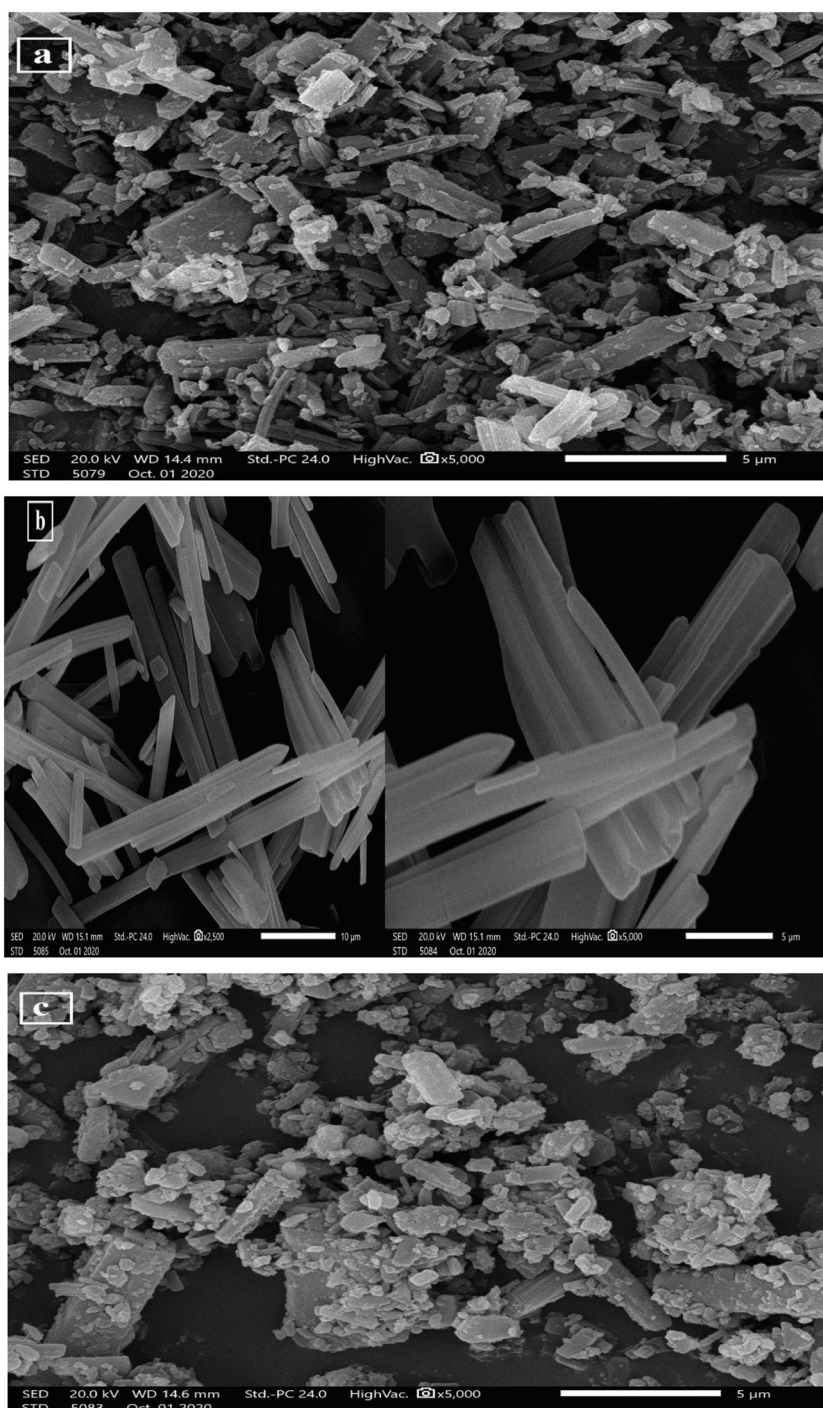


Fig. 4. SEM microphotographs of **a** atorvastatin, **b** ezetimibe (at two different magnifications), and **c** the co-processed dose ratio

ezetimibe and atorvastatin co-processed form on the total serum cholesterol concentration and the integrity of liver tissues. This was compared to the effect of oral administration of each drug individually or in the form of physical mixture. The effects of the tested formulations on total cholesterol concentration are shown in Fig. 6. The total concentration of cholesterol of untreated mice was 70.7 ± 7.1 mg/dl. This concentration correlates with the reported normal values of the animal (47). Intra-peritoneal administration of poloxamer resulted in significant increase ($p < 0.05$) in total cholesterol

concentration in group II (255.7 ± 20.5 mg/dl) indicating successful induction of hyperlipidemia and kept as positive control. Oral administration of either atorvastatin or ezetimibe individually for group III and IV, respectively, resulted in slight reduction in total cholesterol concentration (Fig. 6). Co-administration of both drugs in the form of physical mixture for group V resulted in additional reduction in cholesterol concentration compared with each drug individually and this can be attributed to the synergistic pharmacological effect of atorvastatin and ezetimibe. This synergistic

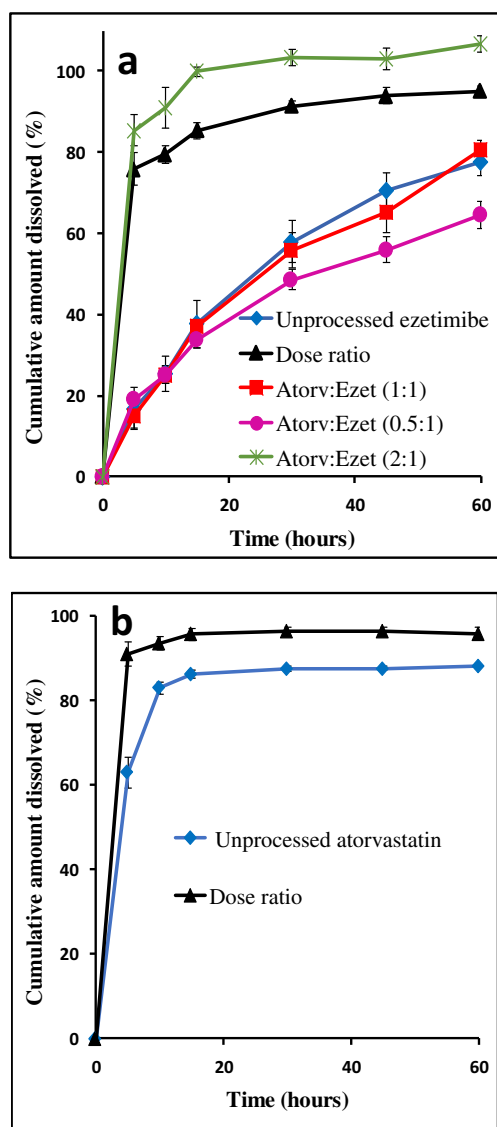


Fig. 5. The dissolution profiles of pure drugs and the tested formulations. **a** Dissolution profiles of ezetimibe and **b** dissolution profiles of atorvastatin

pharmacological effect was previously reported in literatures as atorvastatin is able to inhibit HMG-CoA reductase (the rate-limiting enzyme in cholesterol biosynthesis in liver) and ezetimibe that inhibits cholesterol absorption from small intestine (48). Oral administration of co-processed form of

atorvastatin and ezetimibe for group VI produced a significant enhancement in their pharmacological effect as revealed from the significant reduction ($p < 0.05$) in the total cholesterol concentration (84 ± 14.8 mg/dl). This concentration is approximately similar to the normal level as in group I (negative control). The efficacy of co-processed mixture was superior compared with the corresponding physical mixture suggesting enhanced oral bioavailability of both drugs after co-processing. The enhanced pharmacological effect is parallel to the enhanced dissolution rate after co-processing. This reflects good *in vitro in vivo* correlation. Polymer-assisted dissolution enhancement of atorvastatin ezetimibe mixture has been shown to augment oral bioavailability of both drugs (24). In addition, the oral bioavailability of atorvastatin significantly enhanced after processing the drug in the form of surface stabilized nanocrystals. This enhancement was attributed to the increase in drug solubility (10). Similarly, the oral bioavailability of ezetimibe greatly improved after enhancing the drug dissolution rate by being formulated in the form of amorphous solid dispersion nanoparticles or self-micellizing solid dispersions system (21, 49). These data indicate that the dissolution rate of atorvastatin and ezetimibe is the rate limiting step for drugs oral absorption and hence their bioavailability.

The enhanced pharmacological activity was confirmed further via histopathological examination of liver samples. This investigation was performed taking into consideration the destructive effect of cholesterol on liver tissues (50, 51). The goal was to monitor the protective effects of the developed formulation. The micrographs of H&E-stained liver samples are shown in Fig. 7. The micrograph of the liver tissues for group I (negative control) revealed normal histology of liver tissue showing proper arrangement of liver cells around the central vein (arrow) (Fig. 7). Poloxamer-induced hyperlipidemia compromised the liver histology to reveal clear liver steatosis. This was associated with diffuse hepatic vacuolation consistent with glycogen infiltration. The photomicrograph also showed signs of moderate fatty vacuolation (arrow) in addition to focal coagulative necrosis (arrowhead) (Fig. 7). Oral administration of atorvastatin alone resulted in moderate improvement, but the liver tissues showed focal hepatic vacuolation (arrows) (Fig. 7). Mild improvement was also recorded in the animal group receiving ezetimibe alone which showed midzonal and periportal hepatic vacuolation (arrows) (Fig. 7). Administration of atorvastatin and ezetimibe physical mixture slightly decreased the hepatic vacuolation in liver tissues (arrows) (Fig. 7) while the administration of atorvastatin and ezetimibe co-processed

Table II. The Dissolution Efficiency and Q5 Values of Pure Drugs and the Tested Co-processed Formulations

Formulation	Ezetimibe		Atorvastatin	
	Q5(%)	Dissolution efficiency (%)	Q5 (%)	Dissolution efficiency (%)
Unprocessed drug	16.8 \pm 5.3	51.6 \pm 4.4	62.9 \pm 3.7	81.3 \pm 0.33
Atorv:Ezet (0.5:1)	18.9 \pm 1.1	43.5 \pm 2.3	ND	ND
Atorv:Ezet (1:1)	14.9 \pm 2.8	49.8 \pm 2.3	ND	ND
Atorv:Ezet (2:1)	85.3 \pm 3.9	96.3 \pm 1.9	ND	ND
Dose ratio	75.9 \pm 3.97	85.3 \pm 1.6	90.97 \pm 2.95	91.4 \pm 1.3

Values are presented as mean \pm S.D, $n = 3$. ND is not determined

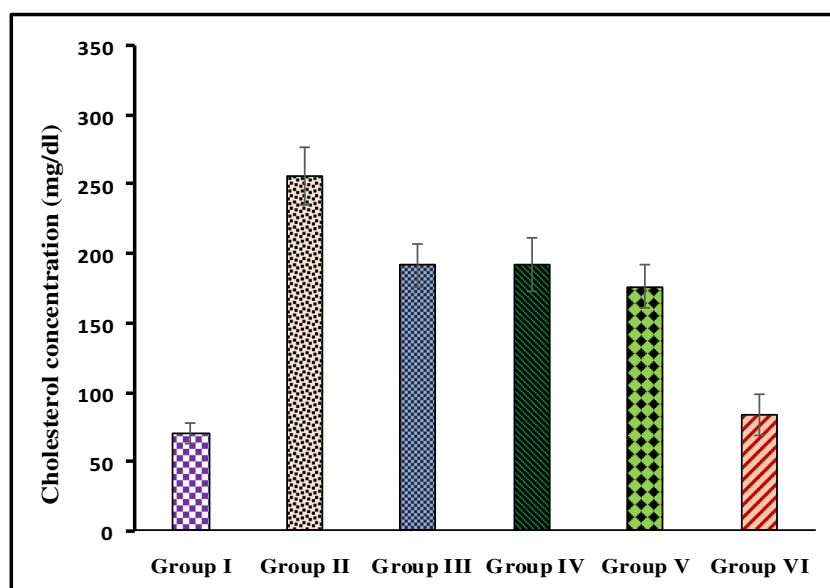


Fig. 6. Total cholesterol concentration in the collected blood samples for each group presented as mean (mg/dl) \pm standard error

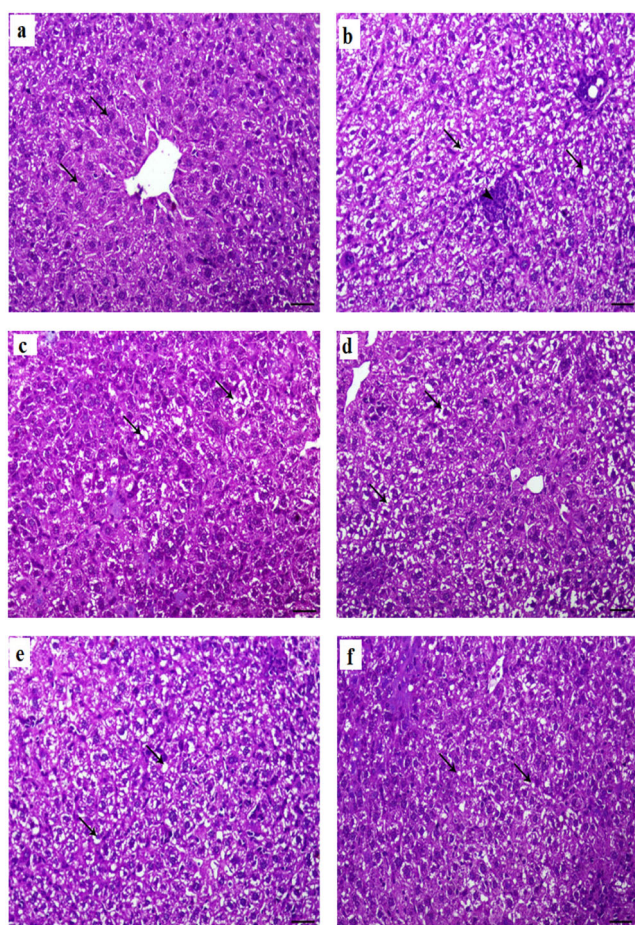


Fig. 7. Micrographs of stained liver sections using H&E stain; **a** group I negative control, **b** group II positive control, **c** group III receiving atorvastatin, **d** group IV receiving ezetimibe, **e** group V receiving physical mixture of both drugs, and **f** group VI receiving co-processed drugs

form resulted in marked decrease in hepatic vacuolation (arrows) (Fig. 7). These results are compatible with the recorded effect of the administered drugs on the total serum cholesterol concentration.

CONCLUSION

Ethanol-aided wet co-processing of atorvastatin with ezetimibe developed eutectic mixture with fast liberation of both drugs. Co-administration of both drugs synergistically augmented the pharmacological effects compared to that recorded from administration of single drug. The co-processed mixture was more efficient than the physical mixture indicating a reflection of enhanced dissolution rate on the recorded *in vivo* availability which was assessed pharmacologically.

REFERENCES

1. Alshaikh RA, Essa EA, El Maghraby GM. Eutectia for enhanced dissolution rate and anti-inflammatory activity of nonsteroidal anti-inflammatory agents: caffeine as a melting point modulator. *Int J Pharm.* 2019;563:395–405.
2. Abdelquader MM, Essa EA, El Maghraby GM. Inhibition of co-crystallization of Olmesartan medoxomil and hydrochlorothiazide for enhanced dissolution rate in their fixed dose combination. *AAPS PharmSciTech.* 2019;20(3):1–12. <https://doi.org/10.1208/s12249-018-1207-9>.
3. Riekes MK, Engelen A, Appeltans B, Rombaut P, Stulzer HK, Van den Mooter G. New perspectives for fixed dose combinations of poorly water-soluble compounds: a case study with ezetimibe and lovastatin. *Pharm Res.* 2016;33(5):1259–75.
4. Wang FY, Zhang Q, Zhang Z, Gong X, Wang JR, Mei X. Solid-state characterization and solubility enhancement of apremilast drug–drug cocrystals. *Cryst Eng Comm.* 2018;20(39):5945–8.
5. Górnaiak A, Irzabek HC, Złocińska A, Karolewicz B. Physico-chemical and dissolution properties of ezetimibe–aspirin binary system in development of fixed-dose combinations. *J Therm Anal Calorim.* 2020. <https://doi.org/10.1007/s10973-020-09543-9>.

6. Rodde MS, Divase GT, Devkar TB, Tekade AR. Solubility and bioavailability enhancement of poorly aqueous soluble atorvastatin: in vitro, ex vivo, and in vivo studies. *Biomed Res Int*. 2014;2014:463895–10. <https://doi.org/10.1155/2014/463895>.
7. Prabhu P, Patravale V. Dissolution enhancement of atorvastatin calcium by co-grinding technique. *Drug Deliv and Transl Res*. 2016;6:380–91.
8. Zhang HX, Wang JX, Zhang ZB, Le Y, Shen ZG, Chen JF. Micronization of atorvastatin calcium by antisolvent precipitation process. *Int J Pharm*. 2009;5:374(1-2):106-113.
9. Kurakula M, El-Helw AM, Sobahi TR, Abdelaal MY. Chitosan based atorvastatin nanocrystals: effect of cationic charge on particle size, formulation stability, and in-vivo efficacy. *Int J Nanomedicine*. 2015;10:321–34.
10. Sharma M, Mehta I. Surface stabilized atorvastatin nanocrystals with improved bioavailability, safety and antihyperlipidemic potential. *Sci Rep*. 2019;9:16105. <https://doi.org/10.1038/s41598-019-52645-0>.
11. Al-Kazemi R, Al-Basarah Y, Nada A. Dissolution enhancement of atorvastatin calcium by cocrystallization. *Adv Pharm Bull*. 2019;9:559–70.
12. Shayanfar A, Ghavimi H, Hamishekar H, Jouyban A. Coamorphous atorvastatin calcium to improve its physicochemical and pharmacokinetic properties. *J Pharm Pharm Sci*. 2013;16(4):577–87.
13. Shamsuddin FM, Ansari SH, Ali J. Atorvastatin solid dispersion for bioavailability enhancement. *J Adv Pharm Technol Res*. 2016;7(1):22–6.
14. Shaker MA, Elbadawy HM, Shaker MA. Improved solubility, dissolution, and oral bioavailability for atorvastatin-Pluronic(R) solid dispersions. *Int J Pharm*. 2020;574:118891. <https://doi.org/10.1016/j.ijpharm.2019.118891>.
15. Yeom DW, Song YS, Kim SR, Lee SG, Kang MH, Lee S, et al. Development and optimization of a self-microemulsifying drug delivery system for atorvastatin calcium by using D-optimal mixture design. *Int J Nanomedicine*. 2015;10:3865–77.
16. Kassem AM, Ibrahim HM, Samy AM. Development and optimisation of atorvastatin calcium loaded self-nanoemulsifying drug delivery system (SNEDDS) for enhancing oral bioavailability: in vitro and in vivo evaluation. *J Microencapsul*. 2017;34(3):319–33.
17. Hashem FM, Al-Sawahli MM, Nasr M, Ahmed OA. Optimized zein nanospheres for improved oral bioavailability of atorvastatin. *Int J Nanomedicine*. 2015;10:4059–69.
18. Zidan MF, Ibrahim HM, Afouna MI, Ibrahim EA. In vitro and in vivo evaluation of cyclodextrin-based nanospheres for enhancing oral bioavailability of atorvastatin calcium. *Drug Dev Ind Pharm*. 2018;44(8):1243–53.
19. Phan BA, Dayspring TD, Toth PP. Ezetimibe therapy: mechanism of action and clinical update. *Vasc Health Risk Manag*. 2012;8:415–27.
20. Sharma N, Singh S. Central composite designed ezetimibe solid dispersion for dissolution enhancement: synthesis and in vitro evaluation. *Ther Deliv*. 2019;10(10):643–58.
21. Torrado-Salmerón C, Guarnizo-Herrero V, Cerezo-Garreta J, Torrado Durán G, Torrado-Santiago S. Self-micellizing technology improves the properties of ezetimibe and increases its effect on hyperlipidemic rats. *Pharmaceutics*. 2019;11:647. <https://doi.org/10.3390/pharmaceutics11120647>.
22. Bandyopadhyay S, Katare OP, Singh B. Optimized self nanoemulsifying systems of ezetimibe with enhanced bioavailability potential using long chain and medium chain triglycerides. *Colloids Surf B: Biointerfaces*. 2012;1(100):50–61.
23. Srivalli KM, Mishra B. Improved aqueous solubility and antihypercholesterolemic activity of ezetimibe on formulating with hydroxypropyl- β -cyclodextrin and hydrophilic auxiliary substances. *AAPS PharmSciTech*. 2016;17(2):272–83.
24. Jahangiri A, Barzegar-Jalali M, Garjani A, Javadzadeh Y, Hamishehkar H, Asadpour-Zeynali K, et al. Evaluation of physicochemical properties and in vivo efficiency of atorvastatin calcium/ezetimibe solid dispersions. *Eur J Pharm Sci*. 2016;82:21–30.
25. Jahangiri A, Barzegar-Jalali M, Javadzadeh Y, Hamishehkar H, Adibkia K. Physicochemical characterization of atorvastatin calcium/ezetimibe amorphous nano-solid dispersions prepared by electrospraying method. *Artif Cells Nanomed Biotechnol*. 2017;45(6):1–8.
26. Hwang KM, Park SA, Kim JY, Park CW, Rhee YS, Park ES. Formulation and in vitro evaluation of self-microemulsifying drug delivery system containing fixed-dose combination of atorvastatin and ezetimibe. *Chem Pharm Bull (Tokyo)*. 2015;63(6):423–30.
27. Alshaikh RA, Essa EA, El Maghraby GM. Preparation of stabilized submicron fenofibrate crystals on niacin as a hydrophilic hydrotropic carrier. *Pharm Dev Technol*. 2020;25(2):168–77.
28. Khan KA. The concept of dissolution efficiency. *J Pharm Pharmacol*. 1975;27:48–9.
29. Chaudhary HR, Brocks DR. The single dose poloxamer 407 model of hyperlipidemia; systemic effects on lipids assessed using pharmacokinetic methods, and its effects on adipokines. *J Pharm Pharm Sci*. 2013;16(1):65–73.
30. Rawal T, Mishra N, Jha A. B Apurva, Tyagi RK., Panchal S, Butani S. Chitosan nanoparticles of gamma-oryzanol: formulation, optimization, and in vivo evaluation of anti-hyperlipidemic activity. *AAPS PharmSciTech*. 2018;19:1894–907.
31. Leon C, Wasan KM, Sachs-Barrable K, Johnston TP. Acute P-407 administration to mice causes hypercholesterolemia by inducing cholesterologenesis and down-regulating low-density lipoprotein receptor expression. *Pharm Res*. 2006;23:1597–607.
32. Whittaker P, Hines FA, Robl MG, Dunkel VC. Hisopathological evaluation of liver, pancreas, spleen, and heart from iron-overloaded Sprague-dawley rats*1,2. *Toxicol Pathol*. 1996;24(5):558–63.
33. Arafa MF, El-Gizawy SA, Osman MA, El Maghraby GM. Sucralose as co-crystal co-former for hydrochlorothiazide: development of oral disintegrating tablets. *Drug Dev Ind Pharm*. 2016;42(8):1225–33.
34. Dey S, Chattopadhyay S, Mazumder B. Formulation and evaluation of fixed-dose combination of bilayer gastroretentive matrix tablet containing atorvastatin as fast-release and atenolol as sustained-release. *Biomed Res Int*. 2014;2014:396106–12. <https://doi.org/10.1155/2014/396106>.
35. Thadkala K, Nanam PK, Rambabu B, Sailu C, Aukunuru J. Preparation and characterization of amorphous ezetimibe nanosuspensions intended for enhancement of oral bioavailability. *Int J Pharm Invest*. 2014;4(3):131–7.
36. Shete G, Puri V. Kumar, Bansal AK. Solid state characterization of commercial crystalline and L amorphous atorvastatin calcium samples. *AAPS PharmSciTech*. 2010;11(2):598–609.
37. Choudhary A, Rana AC, Aggarwal G, Kumar V, Zakir F. Development and characterization of an atorvastatin solid dispersion formulation using skimmed milk for improved oral bioavailability. *Acta Pharm Sin B*. 2012;2:421–8.
38. Mendhe AA, Kharwade RS, Mahajan UN. Dissolution enhancement of poorly water-soluble drug by cyclodextrins inclusion complexation. *Int J App Pharm*. 2016;8(4):60–5.
39. Shevalkar G, Vavia P. Solidified nanostructured lipid carrier (S-NLC) for enhancing the oral bioavailability of ezetimibe. *J Drug Deliv Sci Technol*. 2019;53:101211. <https://doi.org/10.1016/j.jddst.2019.101211>.
40. Zaini E, Wahyuni YS, Halim A, Yuliandra Y. Preparation of eutectic mixture of ketoprofen and nicotinamide for enhanced dissolution rate. *Int J Pharm Sci Rev Res*. 2015;35(1):161–4.
41. Umerska A, Bialek K, Zotova J, Skotnicki M, Tajber L. Anticrystal engineering of ketoprofen and ester local anesthetics: ionic liquids or deep eutectic mixtures? *Pharmaceutics*. 2020;12:368. <https://doi.org/10.3390/pharmaceutics12040368>.
42. Dixit RP, Nagarsenker MS. Formulation and in vivo evaluation of self-nanoemulsifying granules for oral delivery of a combination of ezetimibe and simvastatin. *Drug Dev Ind Pharm*. 2008;34(12):1285–96.
43. Zaini E, Azhari D, Fitriani L. Identification and characterization of solid binary system of quercetin-nicotinamide. *Orient J Chem*. 2016;32(3):1545–50.
44. Araya-Sibaja AM, Vega-Baudrit JR, Guillén-Girón T, Navarro-Hoyos M, Cuffini SL. Drug solubility enhancement through the preparation of multicomponent organic materials: eutectics of lovastatin with carboxylic acids. *Pharmaceutics*. 2019;11:112–28.
45. Kunam V, Suryadevara V, Garikapati DR, Basaveswara V, Mandava R, Sunkara SP. Solubility and dissolution rate

- enhancement of ezetimibe by solid dispersion and pelletization techniques. *Asian J Pharm Clin Res.* 2019;12(3):407–13.
46. Özkan CK, Ozgur E, Kurbanoglu S, Savaser A, Ozkan SA, Yalcin O. Development of a suitable dissolution method for the combined tablet formulation of atorvastatin and ezetimibe by RP-LC Method. *Current Drug Delivery.* 2016;13(3):424–30.
47. Sinulingga S, Putri HOV, Haryadi K, Subandrate. The effect of pindang patin intake on serum cholesterol and LDL levels of male mice (*Mus Musculus L.*). *J Phys Conf Ser.* 2019:1246. <https://doi.org/10.1088/1742-6596/1246/1/012060>.
48. Ma YB, Chan P, Zhang Y, Tomlinson B, Liu Z. Evaluating the efficacy and safety of atorvastatin + ezetimibe in a fixed-dose combination for the treatment of hypercholesterolemia. *Expert Opin Pharmacother.* 2019;20(8):917–28.
49. Ha ES, Kim JS, Baek I, Hwang SJ, Kim MS. Enhancement of dissolution and bioavailability of ezetimibe by amorphous solid dispersion nanoparticles fabricated using supercritical antisolvent process. *J Pharm Investig.* 2015;45(7):641–9.
50. Staprans I, Pan X, Rapp JH, Grunfeld C, Feingold KR. Oxidized cholesterol in the diet accelerates the development of atherosclerosis in LDL receptor- and apolipoprotein E-deficient mice. *Arterioscler Thromb Vasc Biol.* 2000;20:708–14.
51. Kengkoom K, Klinkhamhom A, Sirimontaporn A, Singha O, Ketjareon T, Panavechkijkul Y, et al. Effects on high cholesterol-fed to liver, retina, hippocampus, and Harderian gland in Goto-Kakizaki rat. *Int J Clin Exp Pathol.* 2013;6(4):639–49.

Publisher's Note Springer Nature remains neutral with regard to jurisdictional claims in published maps and institutional affiliations.